Electronic structures of 110 -faceted self-assembled pyramidal InAs/GaAs quantum dots

Lin-Wang Wang, Jeongnim Kim, and Alex Zunger
National Renewable Energy Laboratory, Golden, Colorado 80401
~Received 27 July 1998!

We calculate the electronic structures of pyramidal quantum dots with supercells containing 250 000 atoms, using spin-orbit-coupled, nonlocal, empirical pseudopotentials. We compare the results with previous theoretical calculations. Our calculation circumvents the approximations underlying the conventional effective-mass

electronic states ~Ref. 18!: The adequacy of this linear approximation has not been tested in the case of InAs/GaAs, where large ~7%! strains exist.

~iv! *The neglect or the simplification of the electron-hole Coulomb interaction*: As shown recently,[23] the calculation of Coulomb energies from envelope functions, rather than from microscopic wave functions of the quantum dots overestimates the Coulomb energy by as much as 40%.

Points ~i!–~iv! above suggest that it might be desirable to calculate the electronic structure of quantum dots using a method which has fewer approximations than the conventional **k p** model. Here we offer a treatment that avoids approximations ~i!–~iv!.

In this paper, we study the electronic structure of InAs/GaAs quantum dots using our newly developed atomistic pseudopotential method.[5] This approach describes the potential, the strain, and the wave functions using *atomistic*, rather than continuum models. The potential is given by a superposition of screened atomic pseudopotentials, the strain is calculated from minimizing the atomistic strain energy, and the wave functions are not restricted to envelope functions but retain the microscopic part. Consequently, multiband coupling is not limited, atomic features in the density are resolvable, and the deformation potentials are not linearized, thus avoiding the approximations underlying the **k p** calculations. The approximations that are involved include lack of charge self-consistency and a phenomenological treatment of the size- and position-dependent dielectric screening. The same approach has achieved very good agreement with experiment for free-standing quantum dots, including band gap vs size for Si,[24] InP,[25] and CdSe,[26] high-energy excitonic spectra of InP ~Ref. 27! and CdSe,[22] pressure effects on InP,[28] and exchange splitting in InP ~Ref. 29! and CdSe.[5,30] This approach has also been applied to study embedded nanostructures, including pressure effects on InAs/GaAs quantum dots[31] and a GaAs/AlAs ''Russian doll.''[32] Here we report atomistic calculations ~including the spin-orbit interaction! for large embedded dots ~containing a 250 000 atoms in the supercell!. This is made possible by the development of a parallel computer code on the Cray T3E computer. Here we present the results of this calculation for an InAs/GaAs pyramidal quantum dot, analyzing the electron and hole wave functions in real space, and calculating the polarizations of the interband optical transitions and the size dependence of the confined energy levels. We compare our results with the previous **k p**

Since the electronic states are confined mostly inside the dots, a smaller supercell is adequate for a description of the wave functions. Indeed, the dot-dot interaction due to wave-function overlap is much smaller than the long-range dot-dot interaction due to elastic strain. Consequently, for the purpose of calculating the wave functions, we have removed a few GaAs layers from the original $40a \times 40a \times 50a$ supercell, reducing it to a $28a \times 28a \times 30a$ supercell. The atomic positions of the atoms inside and near the pyramid are kept the same as in the original $40a \times 40a \times 50a$ supercell. The atoms in the periphery layers of the $28a \times 28a \times 30a$ box have been relaxed again, so that a smooth, periodic boundary condition can be formed. The single-particle electronic levels calculated ~by the method to be described below! using this reduced supercell differ by less than 0.1 meV from those obtained using the original $40a \times 40a \times 50a$ supercell, although the saving in computational effort is substantial. We emphasize that the shapes of the dot and wetting layer are ''inputs'' to the calculation, and any choice can be entertained.

B. Electronic structure calculations

Having formulated the atomic structures of the dot, wetting layer, and barrier, the electronic structure is obtained next using a direct-diagonalization approach to the single-particle Schrödinger equation in a pseudopotential representation,

$$\left\{ -\frac{1}{2}\nabla^2 + \sum_{n,a} \hat{v}_a(\mathbf{r} - \mathbf{R}_{na}) \right\} c_i(\mathbf{r}) = e_i c_i(\mathbf{r}). \qquad (1)$$

Due to the spin-orbit coupling, the wave function $c_i(\mathbf{r})$ is complex and has both spin-up and spin-down components. $\mathbf{R}_{na}$ denotes the positions of the nth atom of type a, determined from the strain minimization described in Sec. II A above. $\hat{v}_a(\mathbf{r} - \mathbf{R}_{na})$ is the screened pseudopotential[41] of atom type a. It contains a local part and a nonlocal spin-orbit interaction part.

Since our calculation is non-self-consistent, we have to construct screened potentials that emulate as much as possible the effects of self-consistency. This is done in two ways. First, the potential for the common anion ~As! is allowed to differ slightly, depending on if its nearest-neighbors are Ga or In ~Table I!. Second, we introduce in the potential $\hat{v}_a^{\mathrm{loc}}(\mathbf{r} - \mathbf{R}_{na})$ a dependence on the *local* atomic environment, e.g., the hydrostatic strain $\mathrm{Tr}(e)$ of the atoms at $\mathbf{R}_{na}$,

$$v_a^{\mathrm{loc}}(r;e) = v_a^{\mathrm{eq}}(r;0)(1 + g_a \mathrm{Tr}(e)), \qquad (2)$$

where g_a is a fitting parameter. The zero strain potential $v_a^{\mathrm{eq}}(r;0)$ is expressed in reciprocal space q as

$$v(q) = (a_0(q^2 - a_1)/(a_2 e^{a_3 q^2} - 1)). \qquad (3)$$

The local hydrostatic strain $\mathrm{Tr}(e)$ for a given atom at $\mathbf{R}$ is defined as $V_R/V_0 - 1$, where V_R is the volume of the tetrahedron formed by the four atoms bonded to the atom at $\mathbf{R}$. V_0 is the volume of that tetrahedron in the unstrained condition ~bulk InAs or GaAs!. The explicit dependence of the pseudopotential on strain is a feature necessitated by the requirement to fit the local density approximation ~LDA!-derived self-consistent absolute deformation potential of the valence band.[41] In the absence of this term, one obtains an incorrect sign ~positive, instead of negative! for the deformation potential of the valence band.

The nonlocal spin-orbit interaction $\hat{v}_a^{\mathrm{nonloc}}$ in $\hat{v}_a(\mathbf{r} - \mathbf{R}_{na})$ is described by a Kleinmen-Bylander separable form[42]

$$\hat{v}_a^{\mathrm{nonloc}} = b_a ($$

the folded spectrum method,[45] which solves for only a few states near the valence-band maximum ~VBM! and conduction-band minimum ~CBM!. The computational time of the folded spectrum method scales linearly with the number of atoms. Using a parallelized code on a Cray T3E machine, we are able to calculate a 250 000 atom system within 10 cpu hours on 128 nodes.

III. RESULTS

A. Confined electron and hole levels

We have calculated four conduction states and four valence states for each quantum dot. The four conduction state energies for the pyramid with a base size of b 5 20a are 2 4.4230, 2 4.3305, 2 4.3068, and 2 4.2483 eV ~measured from the vacuum level!, and are labeled from CBM to CBM 1 3, respectively. The four hole-state energies for the same system are at 2 5.3823, 2 5.3926, 2 5.4027, and 2 5.4094 eV and are labeled from VBM to VBM 2 3, respectively. In Fig. 2 , we show the quantum size dependence of the electron and hole energy levels. The energies are compared with the CBM and VBM of the monolayer-thick wetting layer, which are calculated separately in a coherently strained quantum-well geometry with atomic positions calculated from the VFF model. From Fig. 2 we see that there are at least four bound-electron states for the b 5 20a system, consistent with our previous, non-spin-orbit interaction calculations.[20] The four calculated hole states are well above the VBM of the wetting layer. As the dot size is reduced, the valence-band energies become more negative while the conduction band energies become less negative. As expected, quantum confinement thus causes the number of bound-electron states to decrease as the size of the quantum dot is reduced. As we can see, the number of bound-electron state is reduced to 2 for the b 5 12a pyramid system.[46]

B. Confined wave functionsstate.4

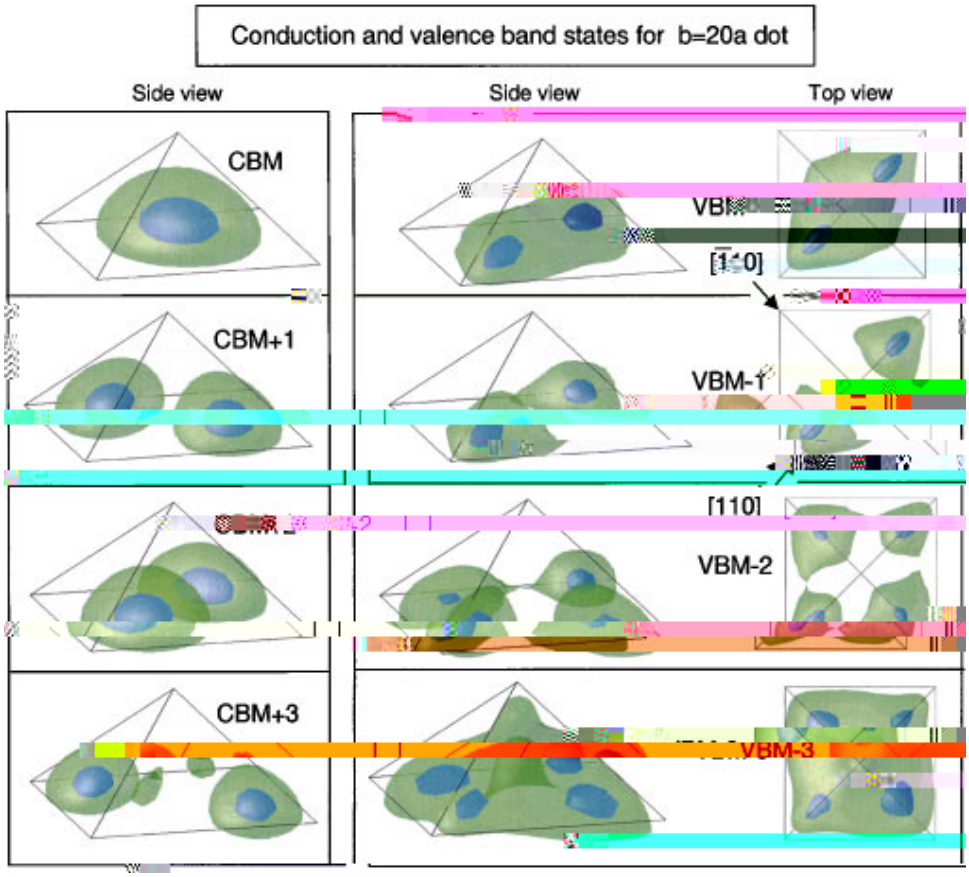

FIG. 3. ~Color! Isosurface plots of the charge densities of the conduction- and valence-band states for the b 5 20a pyramids. The charge density equals the wave-function square, including the spin-up and -down components. The level values of the green and blue isosurfaces equal 0.25 and 0.75 of the maximum charge density, respectively.

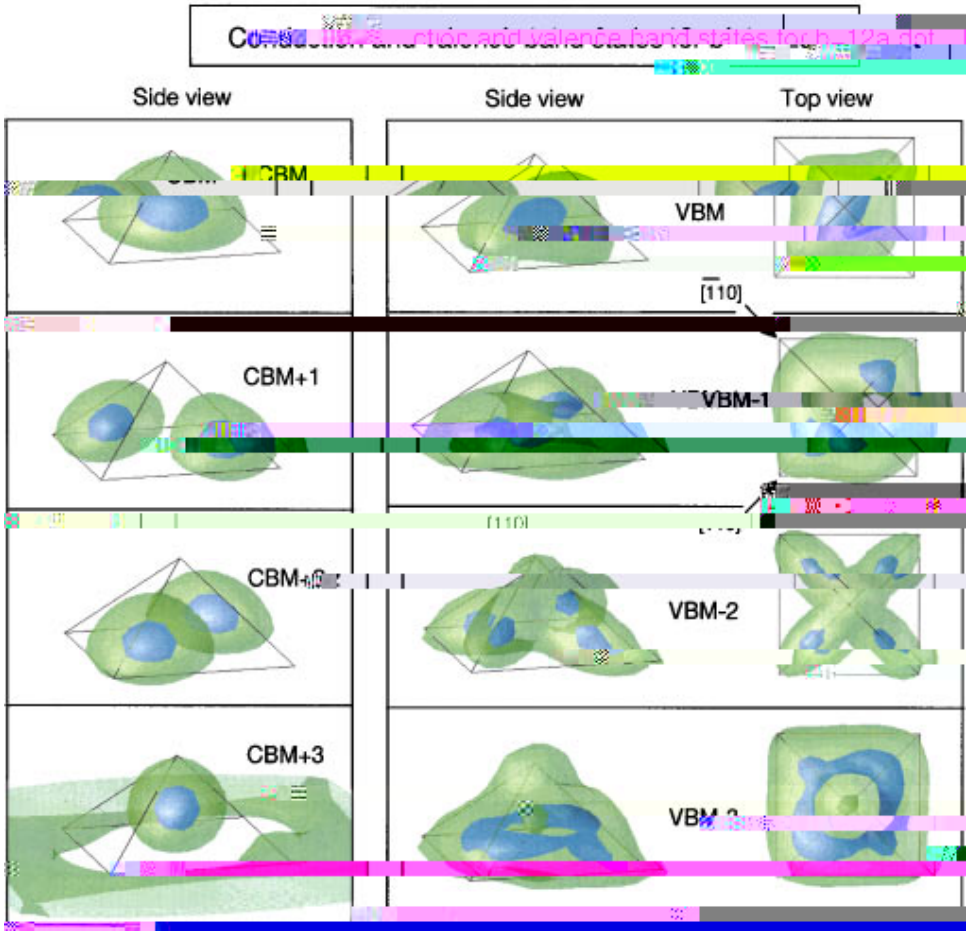

FIG. 4. ~Color! Isosurface plots of the charge densities of conduction- and valence-band states for the b 5 12a pyramids. See the caption of Fig. 3 for more details.

recent eight-band **k** **p** calculation by Pryor,[18] the piezoelectric effect only splits the two *p*-like states by 2 meV for the *b* 5 20*a* quantum dot. This is ten times smaller than the splitting caused by the anisotropy of the atomic structure. Thus the piezoelectric effect can be safely neglected.

The CBM 1 3 conduction state in the *b* 5 20*a* dot is *d* like, with two nodal planes along the @110# direction. This is also true for the CBM 1 3 state in the *b* 5 16*a* and the 18*a* based dots. However, for the *b* 5 12*a* dot, the CBM 1 3 state is resonant with a wetting layer state, so the wave function leaks into the wetting layer.

In a previous study,[20] we showed the isosurface plots for conduction states and valence states calculated without the spin-orbit interactions. As expected, the current calculation ~which includes the spin-orbit interaction! yields almost the same results for the conduction states, but different results for the valence states. For example, the VBM calculated with spin-orbit interaction has fewer structures than its counterpart in the non-spin-orbit interaction calculation. Note that, although the corresponding isosurfaces of the valence states of the *b* 5 20*a* and *b* 5 12*a* quantum dots look different, they are actually qualitatively the same state with the same polarization properties.[47] Thus, as the size of the pyramid changes, there is no valence-band state crossing.

An interesting result obtained from our atomistic calculation is that while the conduction states of the dot are made essentially of single-envelope functions, and so can be classified as being *s* like ~CBM!, *p* like (CBM 1 1 and CBM 1 2), *d* like (CBM 1 3), etc., the valence states represent such a strong band mixing that they cannot be classified according to their nodal structure as being *s* like, *p* like, etc. *In fact, our calculated valence state of Figs. 3 and 4 show no nodal planes.*[47] We conclude that the valence states cannot be classified according to their nodal structures being *s* like, *p* like, etc. The approximation[15,48] of using a single heavy-hole band to describe the valence state is thus qualitatively incorrect. This is because, unlike the case of one dimensional quantum well or superlattice, in dots the heavy hole and light hole are mixed very strongly so as to be inseparable.

C. Electron-hole Coulomb energies

The Coulomb interaction between the valence states and the conduction states is calculated as

$$J_{i,j} 5 \int \int$$

both @110# and @$\overline{1}$10# polarizations, but forbidden for *z* polarization, while the transitions to the second and third (*p*-like! conduction bands are allowed in *z* polarization. The transition from the second valence band to the CBM is rather weak, and is *z* polarized. Table IV shows the following. ~i! All valence-to-conduction transitions are allowed. ~ii! The strongest transition occurs along the @110# [u_1 and @$\overline{1}$10# [u_2 directions. ~iii! There are significant polarization anisotropies between u_1 and u_2 directions. Defining the intensity ratio along the two substrate directions as

$$\frac{I_{ij}@110\#}{I_{ij}@\overline{1}10\#} 5 \frac{|\wedge c_{i,v}|P_{[110]}|\, c_{j,c}\&|^2}{|\wedge c_{i,v}|P_{[\overline{1}10]}|\, c_{j,c}\&|^2} \qquad \text{~6!}$$

guing that the experimental shape is a square-based pyramid, this calculation does demonstrate that the measured polariza-

; 10-meV energy difference. These nonlinear strain effects are not represented in the current eight-band **k p** models.[13–15,17–19] In our pseudopotential model, we have taken into account the nonlinear effects by fitting to the LDA band structures at a few different strains relevant to the pyramidal quantum dot. Since our pseudopotential of Eq. ~3! is close to the *ab initio* potential, it represents the nonlinear effects in an intrinsic way.[44,41]

IV. SUMMARY

We have used the pseudopotential approach, including spin-orbit interactions, to calculate the electronic structure of square-based pyramidal quantum dots. We find the following. ~1! While the conduction bands are essentially derived from well-defined single-envelope functions, the valence states show massive interband coupling. As a result, the valence states have no nodal planes and therefore cannot be classified as s, p, and d states. As a consequence, the optical spectrum of such dots cannot be interpreted using simplified descriptions ~successful in quantum wells! that include only heavy-hole states or only light-hole states. Another consequence of the strong coupling between hole states is that the lowest interband transition has a very different intensity along each of the two in-plane substrate directions @110# and @$\bar{1}$10#. This anisotropy exists even in the absence of strain ~ thus reflecting pure band coupling! and is absent in typical **k p** calculations. ~2! There are > 4 bound electron states for the b 5 20a pyramidal quantum dot. This number is larger than that obtained in the **k p** model, and consistent with the current experimental results. The energy splitting between the p-like conduction bands found in the present study is a factor of 2 larger than the **k p** results. ~3! The current method and the **k p** method appear to have different valence states or different orders of the valence states.

ACKNOWLEDGMENTS

The authors would like to thank A. J. Williamson for

[36] H. Lee, R. Lowe-Webb, W. Yang, and P. C. Sercel, Appl. Phys. Lett. **72**, 812 ~1998!.
[37] M. Grundmann, J. Christen, N. N. Ledentsov, J. Böhrer, D. Bimberg, S. S. Ruvimov, P. Werner, U. Richter, U. Gösele, J. Heydenreich, V. M. Ustinov, A. Yu. Egorov, A. E. Zhukov, P. S. Kop'ev, and Zh. I. Alferov, Phys. Rev. Lett. **74**, 4043 ~1995!.
[38] C. Pryor, J. Kim, L. W. Wang, A. J. Williamson, and A. Zunger, J. Appl. Phys. **83**, 2548 ~1998!.
[39] P. Keating, Phys. Rev. **145**, 637 ~1966!.
[40] R. Martin, Phys. Rev. B **1**, 4005 ~1970!.
[41] A. J. Williamson, J. Kim, L. W. Wang, S. H. Wei, and A. Zunger ~unpublished!.
[42] L. Kleinman and D. M. Bylander, Phys. Rev. Lett. **48**, 1425 ~1982!.
[43] Equation ~4! is implemented in real space, on a fast Fourier transform grid of the wave function c_i. The $|p_x\&$, $|p_y\&$, and $|p_z\&$ reference functions are approximated by x, y, and z times a spherical Bessel function $j_1(4.493r/r_{cut})$, which has its first node at $r 5 r_{cut}$. The reference functions outside r_{cut} are set to zero. We have used $r_{cut} 5 2.25$ a.u for all In, Ga, and As atoms, deduced from the size ranges of the spin-orbit interaction nonlocal pseudopotentials in the local density approximation.
[44] A smooth energy cutoff ~with a smooth cutoff parameter of 0.8! is used in the current calculation, and is defined in L. W. Wang and A. Zunger, Phys. Rev. B **51**, 17 398 ~1995!.
[45] L. W. Wang and A. Zunger, J. Chem. Phys. **100**, 2394 ~1994!.
[46] According to Fig. 2, the third electron state in the $b 5 12a$ dot is above the wetting layer CBM energy. However, as shown in Fig. 4, this state is a normal *p*-like bound state. This contradiction might result from the finite supercell we used, which has limited wetting layer area, thus pushes the wetting layer CBM energy up. So, in reality, according to Fig. 2, the $b 5 12a$ quantum dot should have only two bound electron states.
[47] Consider the VBM-1 state in Figs. 3 and 4. If we lower the isosurface value from 0.25 to 0.1, the two lumps of the green isosurfaces of the $b 5 20a$ dot in Figs. 3 will be connected to form a doughnut, similar to the isosurface plot of VBM-1 state of the $b 5 12a$ quantum dot shown in Figs. 4. Similarly, the VBM-2 and VBM-3 states change from the $b 5 20a$ plots in Fig. 3 to $b 5 12$